Synthesis and Characterization of Dialdehyde Cellulose/ Silver Composites by Microwave-assisted Hydrothermal Method

Bin Wang,[a] Chang Ma,[a] Lian-Hua Fu,[a] Xing-Xiang Ji,[b] Fan-Chen Jing,[a] Shan Liu,[a,*] and Ming-Guo Ma [a,*]

An easy and environmentally friendly strategy is shown for the synthesis of dialdehyde cellulose/silver nanoparticle composites using dialdehyde cellulose as reducing agent through the microwave-assisted hydrothermal method. The effects of the microwave heating time and temperature on the products were investigated by X-ray powder diffraction (XRD), Fourier transform infrared spectroscopy (FT-IR), field emission scanning electron microscopy (FE-SEM), and thermogravimetric analysis (TGA). The dialdehyde cellulose was found to be an efficient reducing agent for silver ions, and the microwave heating time and temperature played a vital role in the morphologies of the silver nanostructures. The influences of different additional reductants such as ascorbic acid and glucose on the shapes, size-distribution, phase, and crystallinity of the samples were comparatively investigated in detail. This strategy is environmentally friendly, surfactant-free, without any other reducing or stabilizing agent chemicals, and the as-prepared dialdehyde cellulose/silver nanoparticles were more convenient to use in biomedical fields.

INTRODUCTION

Cellulose composites have received attention in recent years due to their properties and wide applications in food packaging, drug release, adsorption, wastewater treatment, sensors, and biomedical fields (Miao and Hamad 2013; Shah *et al.* 2013; Kim *et al.* 2014; Natterodt *et al.* 2017). Cellulose is used as a reinforcing component to fabricate composites with outstanding properties (Huber *et al.* 2012). Composites of modified bacterial cellulose and polyvinylidene fluoride display excellent properties, making them a good electroactive biocomposite candidate (Ummartyotin *et al.* 2017). Cellulose/chitosan composites have potential applications for heavy metals and dye removal in wastewater treatment (Olivera *et al.* 2016). Polyethylene/cellulose nanocrystal composites with improved mechanical properties were prepared using an organic-solvent-free two-step process (Sapkota *et al.* 2017). Among the cellulose composites, cellulose/Ag composites have received special attention due to their high antibacterial properties (Maleki *et al.* 2016).

There has been rapid progress in the preparation of cellulose/Ag composites using various synthetic strategies (Liu *et al*. 2012; Raghavendra *et al*. 2013; Maleki *et al*. 2017). In a previous study, cellulose/Ag nanocomposites were synthesized using fructose and glucose as reducing reagents by the hydrothermal method (Dong *et al*. 2014). Moreover, Ag@Fe_3O_4@cellulose nanocrystals nanocomposites with good adsorption of dye solution and good antibacterial activities were obtained by the microwave-assisted hydrothermal method (Dong *et al*. 2017).

As the most effective antibacterial agent, silver nanoparticles (AgNPs) are exploited in many fields, including wound dressing (deBoer *et al*. 2015; Wu *et al*. 2018), dental material (Slenters *et al*. 2008), textile fabric (Agarwal *et al*. 2015), and food packaging (Becaro *et al*. 2015). AgNPs have good antimicrobial efficacy against bacteria, viruses, and eukaryotic micro-organisms (Gong *et al*. 2007).

Reducing agents are frequently required to prepare AgNPs. The demonstrated reducing agents have included chemical regents, natural polysaccharides, and plants extracts (Ahmed *et al*. 2016; Fu *et al*. 2016a). Among these, natural polysaccharides have excellent features such as chemical stability, biocompatibility, and biodegradation. For example, Emam and EI-Bisi (2014) prepared AgNPs using three different cellulose fibers (viscose, lyocell, and cotton) as removable reductants. Xiong *et al.* (2013) synthesized tunable AgNPs (silver nanospheres and dendritic nanostructures) using cellulose nanocrystals in aqueous solution without employing any other reductants, capping, or dispersing agents.

In a previous study, the AgNPs were prepared using holocellulose as a substrate and reducing agent, and the holocellulose was shown to be more efficient than the typical reducing agents of $NaBH_4$ and ascorbic acid (Fu *et al*. 2016a). The reducibility of the aforementioned cellulose benefited from the reduction because aldehyde groups were removed at one end of its chains. The periodate oxidation of cellulose could cleave the C2 to C3 bond of the glucopyranoside ring, resulting in the formation of two aldehyde groups per unit (dialdehyde cellulose) (Kim *et al*. 2000). Therefore, dialdehyde cellulose should be an excellent reducing agent with great reducibility because of the abundant aldehyde groups, and because dialdehyde cellulose can be removed from the products by facile centrifugation in hot water (Kim *et al*. 2004). However, the synthesis of dialdehyde cellulose/silver nanoparticle composites using dialdehyde cellulose as a reducing agent through the microwave-assisted hydrothermal method has not been reported.

Herein, the dialdehyde cellulose/silver nanoparticle composites were synthesized by a simple and green microwave-assisted hydrothermal method using $AgNO_3$ as reactants and dialdehyde cellulose as the reducing agent in aqueous solution. The effects of the microwave heating time and temperature on the morphology of the products were investigated in detail. The reaction system does not contain any other chemical reducing or stabilizing agents, and if the dialdehyde cellulose was removed from the products by centrifugation for the solubilization of dialdehyde cellulose in hot water, the silver nanoparticles were obtained (Qi *et al*. 2014). The microwave-assisted hydrothermal method has many advantages over conventional heating methods, such as high reaction rate, shorter reaction time, reduced energy consumption, and environmental friendliness (Zhu and Chen 2014; Meng *et al*. 2016). This strategy is environmentally friendly and surfactant-free, avoiding the procedures and cost for the surfactant removal from the product.

EXPERIMENTAL

Materials

All chemicals used in the sample preparation were of analytical grade and used as received without further purification. All experiments were conducted under air atmosphere with deionized water. Microcrystalline cellulose (MCC, molecular weight of 34,843 to 38,894; degree of polymerization (DP), 215 to 240) was obtained from Sinopharm Group Chemical Reagent Co., Ltd., Shanghai, China. Silver nitrate ($AgNO_3$, 98.0%) was purchased from Guangdong Jinhuada Chemical Reagent Co., Ltd. (Beijing, China). Ascorbic acid and glucose were purchased from Beijing Chemical Works (Beijing, China).

Synthesis of Dialdehyde Cellulose/Silver Composites

The dialdehyde cellulose (DAC) was prepared from MCC by the periodate oxidation method (Kim and Kuga 2001; Kim *et al*. 2004). The aldehyde content was determined as 158.8%. For the synthesis of dialdehyde cellulose/silver composites, 0.161 g of DAC and 0.170 g of $AgNO_3$ were added into 30 mL of deionized water under magnetic stirring. The resulting suspension was loaded into an autoclave (60 mL), sealed, and heated in a microwave oven (MDS-6G, Sineo, Shanghai, China) at 150, 180, and 200 °C for 10 or 60 min. The control sample was prepared using MCC instead of DAC, or with the additives of ascorbic acid (0.176 g)/glucose (0.198 g) at 150 °C for 10 min, while maintaining the other conditions. The pH values of the reaction systems before and after microwave-assisted hydrothermal treatment were measured using a pH meter (Sartorius PB-10) under room temperature. The detailed experimental parameters for the preparation of typical samples and the pH value before and after microwave-assisted hydrothermal treatment are shown in Table 1. The product was separated by centrifugation, washed by deionized water and ethanol several times, and dried at 60 °C.

Table 1. The Experimental Parameters for the Preparation of Typical Samples and the pH Value Before and After Microwave-Assisted Hydrothermal Treatment

Sample No.	Cellulose Type	Additives	Temperature (°C) /Time (min)	pH[1]	pH[2]
1	MCC	--	150 / 10	4.81	4.48
2	DAC	--	150 / 10	5.29	2.82
3	DAC	--	150 / 60	5.29	2.77
4	DAC	--	180 / 10	5.29	1.98
5	DAC	--	200 / 10	5.29	1.96
6	DAC	Ascorbic Acid	150 / 10	2.43	2.28
7	DAC	Glucose	150 / 10	5.32	2.84

[1]pH: before microwave-assisted hydrothermal treatment
[2]pH: after microwave-assisted hydrothermal treatment

Characterizations of Dialdehyde Cellulose/Silver Composites

X-ray powder diffraction (XRD) patterns of the as-prepared samples were recorded on a Rigaku D/Max 2200-PC diffractometer (Cu Kα radiation, λ = 1.5405 Å; Tokyo, Japan). Fourier transform infrared (FT-IR) spectroscopic measurements were carried out on Bruker VERTEX 70V spectrophotometer (Karlsruhe, Germany). Field emission scanning electron microscopy (FE-SEM) images were recorded with Hitachi SU8010 (Hitachi, Japan). All samples were Au coated prior to examination by FE-SEM. The size

distributions of the silver particles were obtained from the FE-SEM image using Image J software (https://imagej.nih.gov/ij/). The thermogravimetry analysis (TGA) curves were measured on Shimadzu DTG-60 instrument (Kyoto, Japan) with a heating rate of 10 °C min^{-1} under nitrogen atmosphere, and each sample was weighed between 3 and 5 mg for analysis.

RESULTS AND DISCUSSION

Microstructural Characterization

Figure 1(a) shows the FE-SEM images of the MCC used in this study. MCC displayed a multilayered structure with a smooth surface. After being treated with periodate, the original morphology of the MCC changed, and many channels were observed on the surface of DAC (Fig. 1b). From the FT-IR spectra (Fig. 1c and d), the peak at 881 cm^{-1} is attributed to the hemiacetal and hydrated form, and the peak at 1733 cm^{-1} is the characteristic of carbonyl groups (Kim *et al*. 2000), as shown in Fig. 1d. The appearance of these two peaks demonstrate that the MCC was oxidized to DAC by periodate.
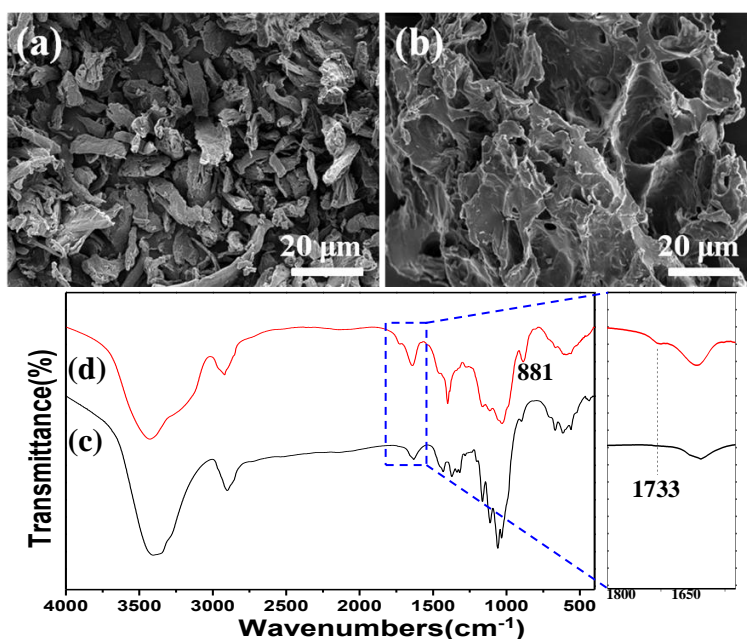

Fig. 1. (a,b) FE-SEM images and (c,d) FT-IR spectra of MCC and DAC: (a,c) MCC, (b,d) DAC.

XRD Characterization

The XRD patterns of the as-prepared samples are shown in Fig. 2. The control sample prepared with MCC showed diffraction peaks around $2\theta = 15.3°$, $21.8°$, and $34.1°$, which can be attributed to the cellulose I (Fig. 2a), and the peak of silver was not observed. In a previous study, a weak peak was determined around $2\theta = 37.9°$ of silver was observed using MCC at a relatively higher temperature of 160 °C for 10 min (Fu *et al*. 2016b). All the samples prepared with DAC exhibited diffraction peaks around $2\theta = 37.9°$, $44.2°$, and $64.3°$, corresponding to the crystal faces of (111), (200), and (220) for the silver with cubic structure (JCPDS: 04 to 0783). With the increasing of reaction time and temperature (Fig. 2c-e), the intensity of the diffraction peaks became stronger, suggesting that prolonging the

reaction time or raising the reaction temperature increased the crystallinity of silver. The DAC was not observed due to its solubilization in hot water (Kim *et al*. 2004). These results from XRD patterns indicated that the DAC was an efficient reducing agent for silver ions.
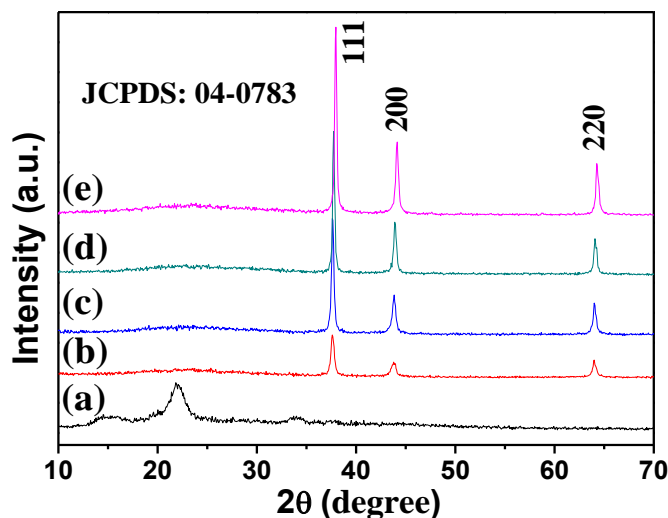
Fig. 2. XRD patterns of (a) the control sample prepared with MCC at 150 °C for 10 min and (b-e) the samples prepared with DAC at different temperatures for different times: (b) 150 °C, 10 min; (c) 150 °C, 60 min; (d) 180 °C, 10 min; (e) 200 °C, 10 min

## Morphology and Size-distribution Characterization

The morphology of the products was investigated with FE-SEM, as shown in Fig. 3. It was difficult to observe AgNPs for the control sample prepared with MCC (Fig. 3a and b), which was consistent with the result in the XRD pattern (Fig. 2a), where the diffraction peak of silver could not be observed.
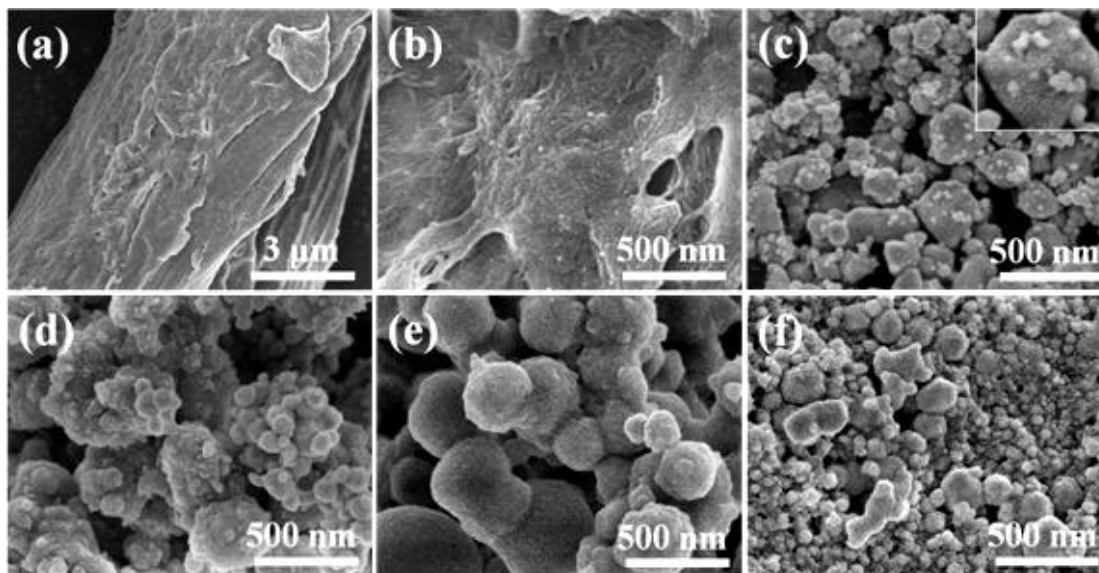
Fig. 3. FE-SEM images of (a,b) the control sample prepared with MCC at 150 °C for 10 min and (c-f) the samples prepared with DAC at different temperatures for different times: (c) 150 °C, 10 min; (d) 150 °C, 60 min; (e) 180 °C, 10 min; (f) 200 °C, 10 min

When the products were prepared with DAC, the silver nanostructures with different morphologies were observed (Fig. 3c-f). For example, the irregular blocks with nanoparticles attached on the surface were obtained at 150 °C for 10 min (Fig. 3c). Prolonging the reaction time to 60 min resulted in the product consisting of both the nanoparticles and nanoparticles-assembled spheres (Fig. 3d). When increasing the reaction temperature to 180 °C, the nanosphere-assembled coral-like structures were observed (Fig. 3e). While further increasing the reaction temperature to 200 °C lead to the product being composed of irregular blocks and nanoparticles (Fig. 3f), and these existed independently rather than like the nanoparticles attached to the blocks (Fig. 3c). These results revealed that the microwave heating time and temperature played a vital role in the morphology of AgNPs.

Figure 4 displays the size distributions of the as-prepared samples with DAC at different temperatures for different times. As for the sample obtained at 150 °C for 10 min, it had a size distribution of ~156.8 nm for the irregular blocks (Fig. 4a) and a size distribution of ~24.6 nm for the nanoparticles (Fig. 4b) attached on the surface.
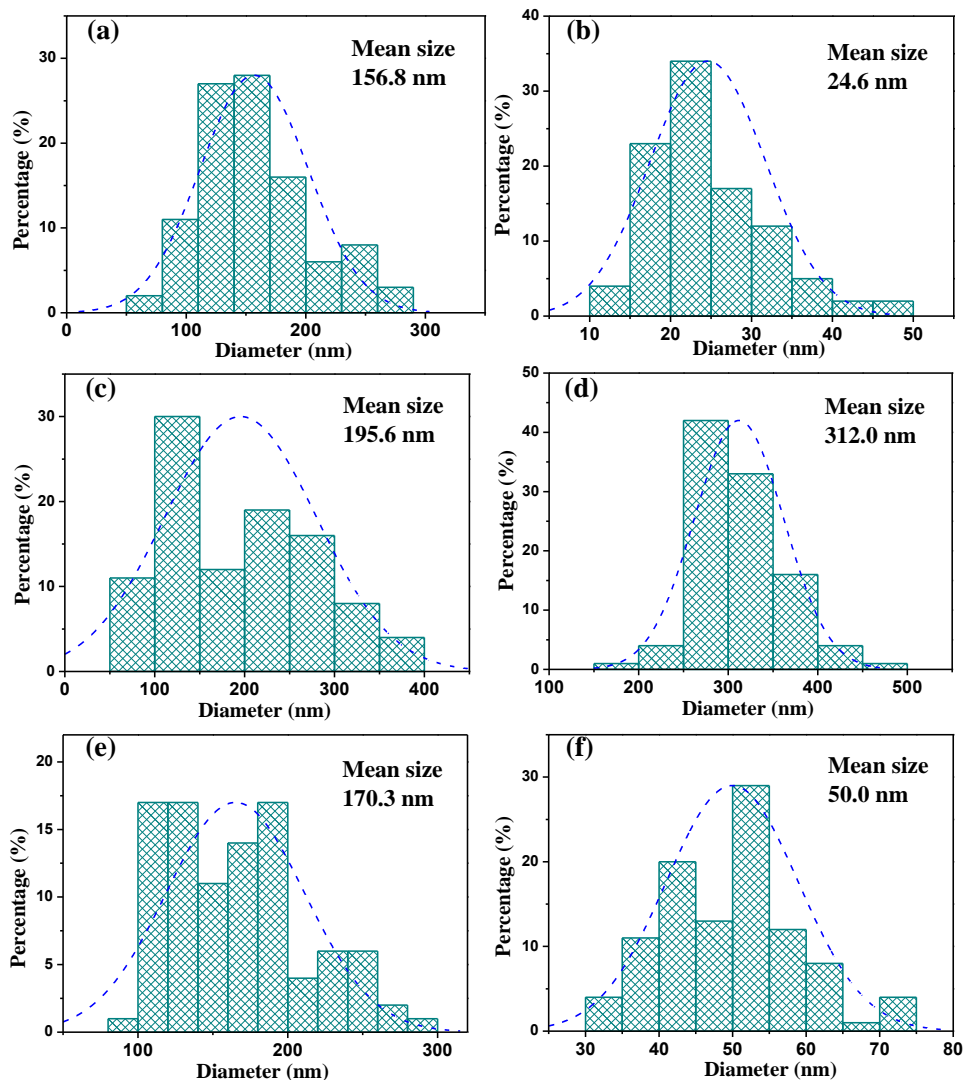

Fig. 4. Size distributions of the samples prepared with DAC at different temperatures for different times: (a,b) 150 °C, 10 min; (c) 150 °C, 60 min; (d) 180 °C, 10 min; (e,f) 200 °C, 10 min

When increasing the reaction time to 60 min, the size distribution increased to ~195.6 nm (Fig. 4c). When increasing the reaction temperature to 180 °C, the nanospheres had a mean size of 312.0 nm (Fig. 4d). By further increasing the reaction temperature to 200 °C, big irregular blocks were obtained with the size of ~170.3 nm (Fig. 4e) and nanoparticles with the size of ~50.0 nm (Fig. 4f). The size distributions of the samples further demonstrated that the microwave heating time and temperature had an effect on the size of AgNPs in the dialdehyde cellulose/silver composites. Moreover, the transport and growth processes in and around the (dialdehyde) cellulose matrix caused the formation of metal particles, inducing the fabrication of nanosphere-assembled coral-like structures with increase size. Of course, the intrinsic mechanism still needs to be explored in the near future.

Thermal Stability Analysis

The thermal stability of the as-prepared products was investigated by TGA. As shown in Fig. 5, the weight loss of the control sample prepared with MCC in the temperature range investigated was about 97.6%. The weight losses were only 7.7%, 10.4%, 14.6%, and 9.4% corresponding to the products prepared with DAC at 150 °C for 10 min, 150 °C for 60 min, 180 °C for 10 min, and 200 °C for 10 min, respectively. These weight losses may have resulted from the degradation of residual DAC in the products, and the small weight loss of the products prepared with DAC revealed the excellent thermal stabilities.
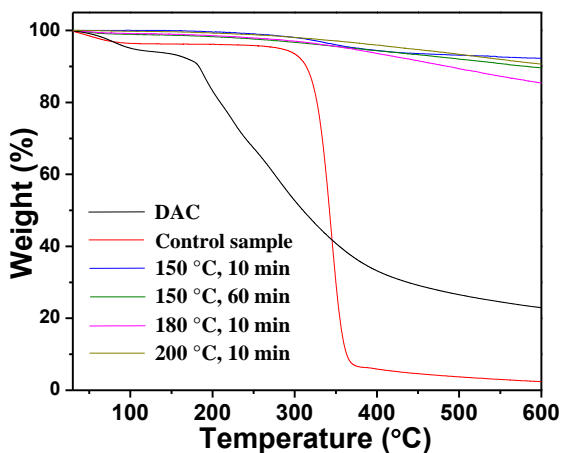

Fig. 5. TGA curves of DAC, the control sample prepared with MCC at 150 °C for 10 min, and the samples prepared with DAC at different temperatures for different times

Formation Mechanism

The formation mechanism of the as-obtained samples can be proposed. Firstly, the MCC was oxidized to DAC by periodate following the literature (Kim and Kuga 2001; Kim *et al.* 2004). The C2 to C3 bond of the glucopyranoside ring was cleaved, resulting in the formation of two reducing aldehyde groups per unit (Fig. 6 (Eq. 1)). Then, the Ag+ ions, which ionized from AgNO$_3$ in an aqueous solution, were reduced to silver by redox reaction with the aldehyde groups (Fig. 6 (Eq. 2)). The pH values of the reaction systems decreased after the microwave-assisted hydrothermal treatment (Table 1), indicating that the acidity of the reaction systems increased. This result confirms that the redox reaction of Ag+ ions and aldehyde groups produced a large number of H+ ions. However, further

research is needed to prove whether or not the aldehyde groups become oxidized into carboxyls. It is notable that the pH value was decreased from 4.81 to 4.48 for the MCC (Table 1), while the peak of silver was not observed in Fig. 1(a). This result may be due to the lower crystallinity of silver, or because the content of silver was too little to detect.
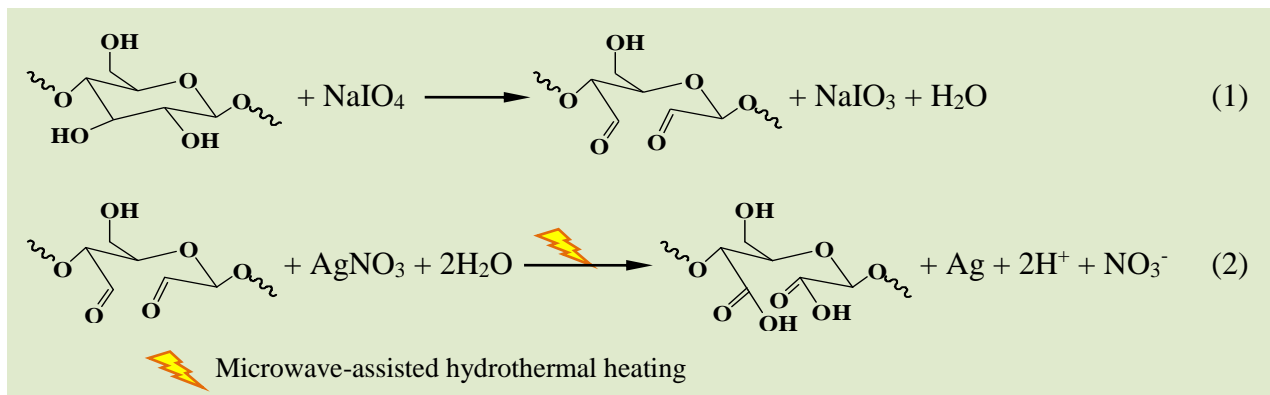
Fig. 6. Scheme of periodate oxidation of cellulose (1) and the reduction of silver nitrate (2)

Influences of Ascorbic Acid and Glucose Analysis

This study also investigated the influences of different additional reductants such as the ascorbic acid and glucose on the as-prepared samples at 150 °C for 10 min. One can see the uniform microspheres (Fig. 7a,b) with a mean size of 1.47 μm using the ascorbic acid as the additional reductant (Fig. 8a). However, when the glucose was used as the additional reductant, both the big irregular blocks and nanoparticles were obtained (Fig. 7c,d), which are similar to the results in Fig. 4(c). This observed the size distribution of ~149.3 nm for the big irregular blocks (Fig. 8b) and ~27.2 nm for the nanoparticles (Fig. 8c).
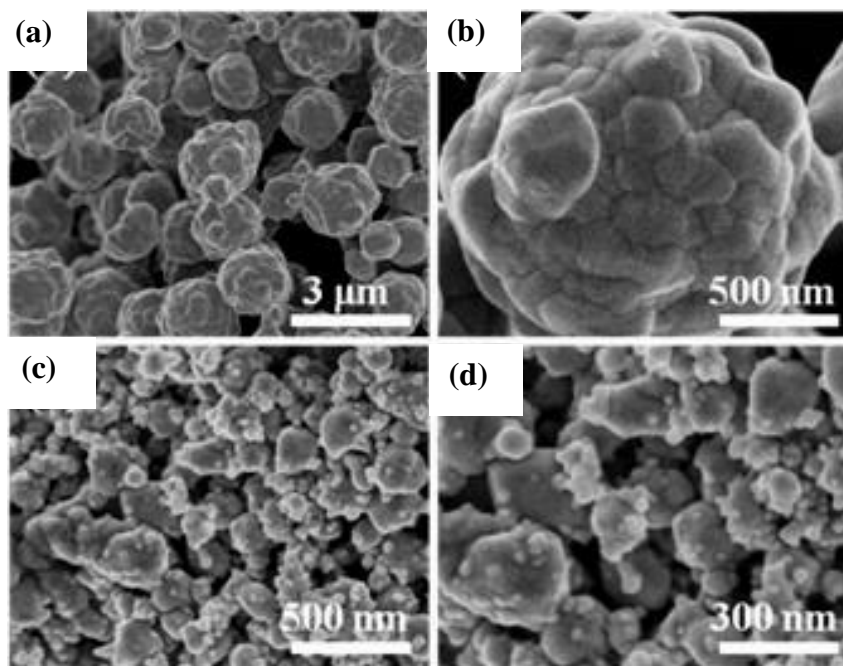
Fig. 7. FE-SEM images of the samples prepared at 150 °C for 10 min with different additional reductants: (a,b) ascorbic acid; (c,d) glucose
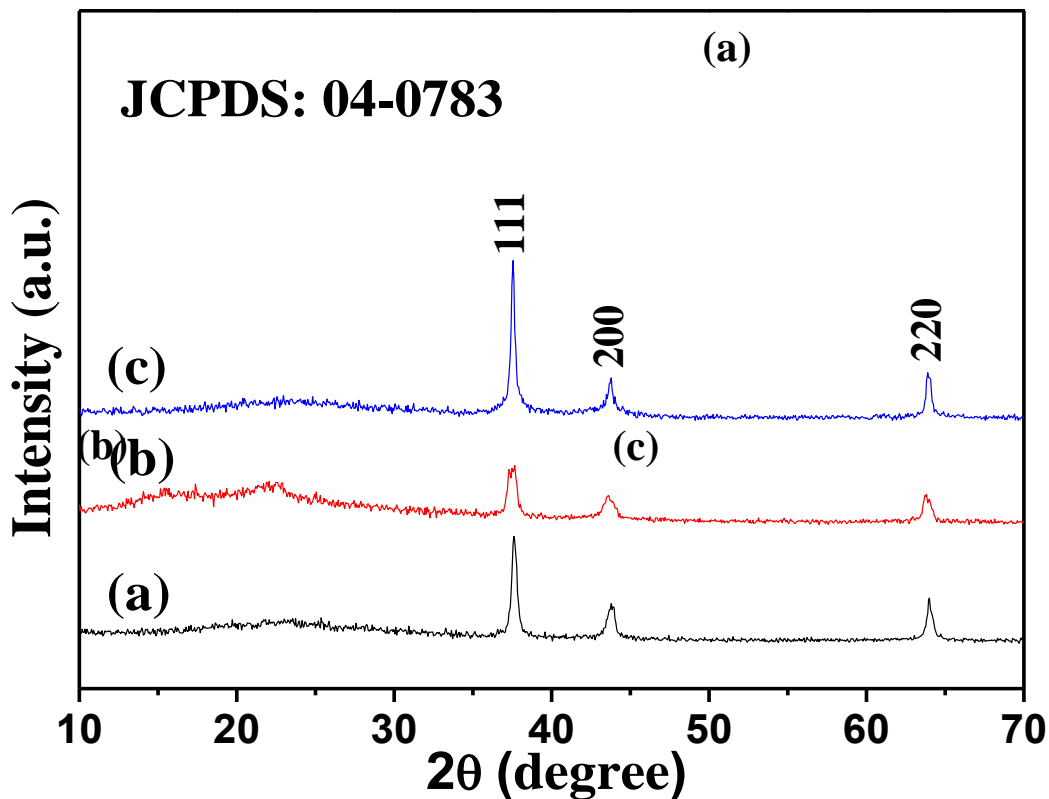
Fig. 8. Size distributions of the samples prepared at 150 °C for 10 min with different additional reductants: (a) ascorbic acid; (b,c) glucose
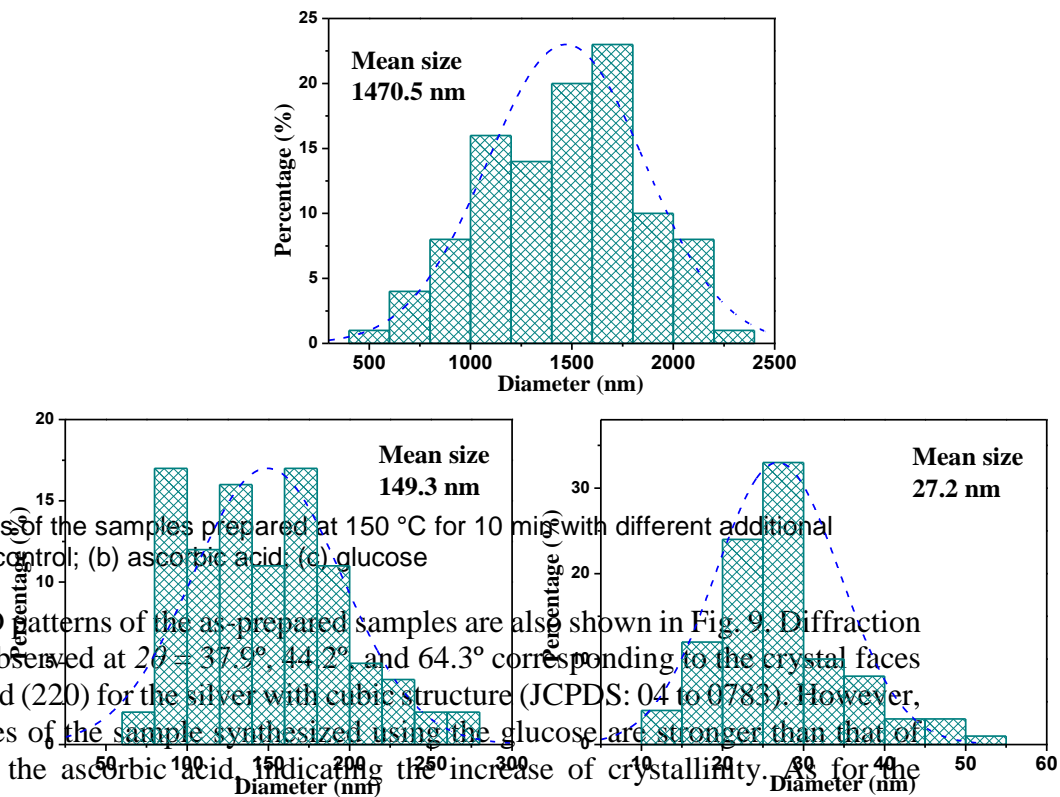

Fig. 9. XRD patterns of the samples prepared at 150 °C for 10 min with different additional reductants: (a) the control; (b) ascorbic acid; (c) glucose

The XRD patterns of the as-prepared samples are also shown in Fig. 9. Diffraction peaks also were observed at $2\theta = 37.9°$, $44.2°$, and $64.3°$ corresponding to the crystal faces of (111), (200), and (220) for the silver with cubic structure (JCPDS: 04 to 0783). However, the peak intensities of the sample synthesized using the glucose are stronger than that of the sample using the ascorbic acid, indicating the increase of crystallinity. As for the

bioresources.com

sample synthesized using the ascorbic acid, the peak of cellulose still could be observed at $2\theta = 21.8°$. The difference of diffraction peaks was due to the reduction ability among the DAC, ascorbic acid, and glucose.

CONCLUSIONS

1. A facile strategy was developed for the synthesis of dialdehyde cellulose /silver nanoparticle composites using the DAC as a reducing agent through the microwave-assisted hydrothermal method.

2. DAC was an efficient reducing agent for silver ions.

3. The microwave heating time and temperature played a vital role in the morphology of the silver nanostructures.

4. The influences of different additional reductants, such as the ascorbic acid and glucose, on the shapes, size-distribution, phase, and crystallinity of the samples were comparatively investigated.

5. This strategy is environmentally friendly and surfactant-free, avoiding the procedures and cost for the surfactant removal from the product.

ACKNOWLEDGMENTS

REFERENCES CITED

Agarwal, R., Garg, N., Kashyap, S. R., and Chauhan, R. P. (2015). "Antibacterial finish of textile using papaya peels derived silver nanoparticles," *Ind. J. Fibr. Text. Res.* 40, 105-107.

Ahmed, S., Ahmad, M., Swami, B. L., and Ikram, S. (2016). "A review on plants extract mediated synthesis of silver nanoparticles for antimicrobial applications: A green expertise," *J. Adv. Res.* 7, 17-28. DOI: 10.1016/j.jare.2015.02.007

Becaro, A. A., Puti, F. C., Correa, D. S., Paris, E. C., Marconcini, J. M., and Ferreira, M. D. (2015). "Polyethylene films containing silver nanoparticles for applications in food packaging: Characterization of physico-chemical and anti-microbial properties," *J. Nanosci. Nanotechnol.* 15, 2148-2156. DOI: 10.1166/jnn.2015.9721

deBoer, T. R., Chakraborty, I., and Mascharak, P. K. (2015). "Design and construction of a silver(I)-loaded cellulose-based wound dressing: Trackable and sustained release of silver for controlled therapeutic delivery to wound sites," *J. Mater. Sci: Mater. in Medic*. 26, 243. DOI: 10.1007/s10856-015-5577-1

Dong, Y. Y., Li, S., Liu, Y. J., Meng, L. Y., and Ma, M. G. (2017). "Ag@Fe$_3$O$_4$@cellulose nanocrystals nanocomposites: Microwave-assisted hydrothermal synthesis, antimicrobial properties, and good adsorption of dye solution," *J. Mater. Sci*. 52, 8219-8230. DOI: 10.1007/s10853-017-1038-1

Dong, Y. Y., Li, S. M., Ma, M. G., Yao, K., and Sun, R. C. (2014). "Compare study cellulose/Ag hybrids using fructose and glucose as reducing reagents by hydrothermal method," *Carbohydr. Polym.* 106, 14-21. DOI: 10.1016/j.carbpol.2014.02.023

Emam, H. E., and EI-Bisi, M. K. (2014). "Merely Ag nanoparticles using different cellulose fibers as removable reductant," *Cellulose*, 21, 4219-4230. DOI: 10.1007/s10570-014-0438-5

Fu, L. H., Deng, F., Ma, M. G., and Yang, J. (2016a). "Green synthesis of silver nanoparticles with enhanced antibacterial activity using holocellulose as a substrate and reducing agent," *RSC Adv.* 6, 28140-28148. DOI: 10.1039/C5RA27421D

Fu, L. H., Liu, B., Meng, L. Y., and Ma, M. G. (2016b). "Comparative study of cellulose/Ag nanocomposites using four cellulose types," *Mater. Lett.* 171, 277-280. DOI: 10.1016/j.matlet.2016.02.118

Gong, P., Li, H. M., He, X. X., Wang, K. M., Hu, J. B., Tan, W. H., Zhang, S. C., and Yang, X. H. (2007). "Preparation and antibacterial activity of Fe_3O_4@Ag nanoparticles," *Nanotechnology,* 18, 604-611. DOI: 10.1088/0957-4484/18/28/285604

Huber, T., Mussig, J., Curnow, O., Pang, S. S., Bickerton, S., and Staiger, M. P. (2012). "A critical review of all-cellulose composites," *J. Mater. Sci.* 47, 1171-1186. DOI: 10.1007/s10853-011-5774-3

Kim, J. H., Mun, S., Ko, H. U., Yun, G. Y., and Kim, J. (2014). "Disposable chemical sensors and biosensors made on cellulose paper," *Nanotechnology* 25, 092001. DOI: 10.1088/0957-4484/25/9/092001

Kim, U. J., and Kuga, S. (2001). "Ion-exchange chromatography by dicarboxyl cellulose gel," *Thermochimica Acta*, 369, 79-85. DOI: 10.1016/S0021-9673(01)00800-7

Kim, U. J., Kuga, S., Wada, M., Okano, T., and Kondo, T. (2000). "Periodate oxidation of crystalline cellulose," *Biomacromolecules* 1, 488-492. DOI: 10.1021/bm0000337

Kim, U. J., Wada, M., and Kuga, S. (2004). "Solubilization of dialdehyde cellulose by hot water," *Carbohydr. Polym.* 56, 7-10. DOI: 10.1016/j.carbpol.2003.10.013

Liu, C., Yang, D., Wang, Y. G., Shi, J. F., and Jiang, Z. Y. (2012). "Fabrication of antimicrobial bacterial cellulose-Ag/AgCl nanocomposite using bacteria as versatile biofactory," *J. Nanopart. Res.* 14, 1084. DOI: 10.1007/s11051-012-1084-1

Maleki, A., Movahed, H., and Paydar, R. (2016). "Design and development of a novel cellulose/gamma-Fe_2O_3/Ag nanocomposite: A potential green catalyst and antibacterial agent," *RSC Adv.* 6, 13657-13665. DOI: 10.1039/c5ra21350a

Maleki, A., Movahed, H., and Ravaghi, P. (2017). "Magnetic cellulose/Ag as a novel eco-friendly nanobiocomposite to catalyze synthesis of chromene-linked nicotinonitriles," *Carbohydr. Polym.* 156, 259-267. DOI: 10.1016/j.carbpol.2016.09.002

Miao, C. W., and Hamad, W. Y. (2013). "Cellulose reinforced polymer composites and nanocomposites: A critical review," *Cellulose* 20, 2221-2262. DOI: 10.1007/s10570-013-0007-3

Meng, L. Y., Wang, B., Ma, M. G., and Lin, K. L. (2016). "The progress of microwave-assisted hydrothermal method in the synthesis of functional nanomaterials," *Mater. Today Chem.* 1-2, 63-68. DOI: 10.1016/j.mtchem.2016.11.003

Natterodt, J. C., Petri-Fink, A., Weder, C., and Zoppe, J. O. (2017). "Cellulose nanocrystals: Surface modification, applications and opportunities at interfaces," *Chimia* 71, 376-383. DOI: 10.2533/chimia.2017.376

Olivera, S., Muralidhara, H. B., Venkatesh, K., Guna, V. K., Gopalakrishna, K., and Kumar, K. Y. (2016). "Potential applications of cellulose and chitosan nanoparticles/composites in wastewater treatment: A review," *Carbohydr. Polym.* 153, 600-618. DOI: 10.1016/j.carbpol.2016.08.017

Qi, C., Zhu, Y. J., and Chen, F. (2014). "Microwave hydrothermal transformation of amorphous calcium carbonate nanospheres and application in protein adsorption," *ACS Appl. Mater. Interfaces*, 6, 4310-4320. DOI: 10.1021/am4060645

Raghavendra, G. M., Jayaramudu, T., Varaprasad, K., Sadiku, R., Ray, S. S., and Raju, K. M. (2013). "Cellulose-polymer-Ag nanocomposite fibers for antibacterial fabrics/skin scaffolds," *Carbohydr. Polym.* 93, 553-560. DOI: 10.1016/j.carbpol.2012.12.035

Sapkota, J., Natterodt, J. C., Shirole, A., Foster, E. J., Weder, C. (2017). "Fabrication and properties of polyethylene/cellulose nanocrystal composites," *Macromol. Mater. Engineer. 302,* 1600300. DOI: 10.1002/mame.201600300

Shah, N., Ul-Islam, M., Khattak, W. A., and Park, J. K. (2013). "Overview of bacterial cellulose composites: A multipurpose advanced material," *Carbohydr. Polym.* 98, 1585-1598. DOI: 10.1016/j.carbpol.2013.08.018

Slenters, T. V., Hauser-Gerspach, I., Daniels, A. U., and Fromm, K. M. (2008). "Silver coordination compounds as light-stable, nano-structured and anti-bacterial coatings for dental implant and restorative materials," *J. Mater. Chem.* 18, 5359-5362. DOI: 10.1039/B813026D

Ummartyotin, S., Thiangtham, S., and Manuspiya, H. (2017). "Strontium-modified bacterial cellulose and a polyvinylidene fluoride composite as an electroactive material," *For. Prod. J.* 67, 288-296. DOI: 10.13073/FPJ-D-16-00041

Wu, C. N., Fuh, S. C., Lin, S. P., Lin, Y. Y., Chen, H. Y., Liu, J. M., and Cheng, K. C. (2018). "TEMPO-oxidized bacterial cellulose pellicle with silver nanoparticles for wound dressing," *Biomacromolecules,* 19, 544-554. DOI: 10.1021/acs.biomac.7b01660

Xiong, R., Lu, C. H., Zhang, W., Zhou, Z. H., and Zhang, X. X. (2013). "Facile synthesis of tunable silver nanostructures for antibacterial application using cellulose nanocrystals," *Carbohydr. Polym.* 95, 214-219. DOI: 10.1016/j.carbpol.2013.02.077

Zhu, Y. J., and Chen, F. (2014). "Microwave-assisted preparation of inorganic nanostructures in liquid phase," *Chem. Rev.* 114, 6462-6555. DOI: 10.1021/cr400366s